PCCP

Accepted Manuscript

ROYAL SOCIETY OF CHEMISTRY

www.rsc.org/pccp

Stabilization of Al(III) solutions by complexation with cacodylic acid: speciation and binding features

Matteo Lari[a], Héctor Lozano[a], Natalia Busto[a], Tarita Biver[b], José M. Leal[a], Saturnino Ibeas, [a] James A. Platts[c], Fernando Secco[b], Begoña Garcia[a]*

[a] *Departamento de Química, Universidad de Burgos, Plaza Misael Bañuelos s/n, 09001 Burgos, Spain*
[b] *Dipartimento di Chimica e Chimica Industriale, Università di Pisa, Via Moruzzi 13, 56124 Pisa, Italy*
[c] *School of Chemistry, Cardiff University, Park Place, Cardiff CF10 3AT, UK.*

*Corresponding author: begar @ubu.es

Abstract Aluminium ion is believed to cause a number of neurological and skeletal disorders in human body. The study of the biological processes and molecular mechanisms that underlie these pathological disorders is rendered a difficult task due to the wide variety of complex species that result from hydrolysis of Al^{3+}ion. In addition, this ion displays a pronounced tendency to precipitate as hydroxide, so that certain complexing agents should be envisaged to stabilize Al(III) solutions near physiological conditions. In this work, we show that the common buffer cacodylic acid (dimethylarsinic acid, HCac) interacts with Al(III) to give stable complexes, even at pH 7. After preliminary analyses of the speciation of the metal ion and also of the ligands, a systematic study of the formation of different Al/Cac complexes at different pH values has been conducted. UV-Vis titrations, mass spectrometry and NMR measurements were performed to enlighten the details of the speciation and stoichiometry of Al/Cac complexes. The results altogether show that Al/Cac dimer complexes prevail, but monomer and trimer forms are also present. Interestingly, it was found that cacodylate promotes formation of such relatively simple complexes, even under conditions where the polymeric form, $Al_{13}O_4(OH)_{24}^{7+}$, should predominate. The results obtained can help to shed some light into the reactivity of aluminium ion in biological environments.

Keywords: Aluminium complexes, dimethylarsinic acid, Al(III) speciation, ^{27}Al-NMR.

1. Introduction

Aluminium ion is prone to forming a variety of hydrolytic species,[1] including the $Al_{13}O_4(OH)_{24}^{7+}$ polymeric form. This ion exhibits certain tendency to precipitate as $Al(OH)_3$, even at relatively acidic pH, and reacts with oxygen-containing ligands.[2,3] Many studies have enlightened the importance of aluminium in biological fluids and its ability to bind biosubstrates, both outside and inside the cell, associating its presence to health diseases.[4-8] The presence of different hydrolytic forms entails involvement of a number of equilibria and, consequently, many other possible complexes. These features render aluminium a very complex system.

Dimethylarsinic (cacodylic) acid, $(CH_3)_2AsOOH$, is largely used to study the interaction of biological molecules with organic dyes or metal ions.[9] Cacodylic acid (HCac, $pK_A = 6.2 \pm 0.1$), with a buffer window ranging pH 5.2 - 7.2,[10-13] is quite a valuable tool to study nucleic acids and proteins under physiological conditions. On the other side, the cacodylate anion is unreactive towards many divalent metal ions;[14] for this reason it can serve to ensure buffer inactivity for many biomolecule/metal ion (or metal complex) systems. On the other hand, there is evidence that the cacodylate anion can bind to metal ions such as Sb(III), Bi(III),[15] Pd(II)[16] and some rare earth metals.[17] Formation of Al(III)/Cac complex[18] and more recently the synthesis of complexes of the dimethylarsinate anion and metal ions of the XIII group (Al, Ga, In, Tl) has been reported.[19] However, to the best of our knowledge, systematic thermodynamic studies of the aluminium/cacodylic acid system in solution under different experimental conditions are still lacking. This work is focused on studying the Al(III)/Cac system at different pH values to infer the nature and strength of the Al(III)/ligand interaction and to assess the possible use of cacodylate to provide Al(III) buffered solutions for biochemical studies at neutral pH.

2. Materials and Methods

2.1. Materials

$Al(ClO_4)_3 \cdot 8H_2O$ solid salt (Fluka) was the aluminium source. Aluminium stock solutions were prepared by dissolving appropriate amounts of the solid in $HClO_4$ aqueous solutions, brought at pH = 2.0 to avoid hydroxide precipitation. Standardization of aluminium stock solutions was carried out through EDTA titrations, using Eriochrome Black-T as an indicator. Briefly, a calibrated excess of EDTA was added to an aliquot of the aluminium solution; the mixture was then boiled and, after addition of acetate buffer (pH = 6.0), it was titrated back with a standardized Zn^{2+} solution. Stock solutions of sodium dimethylarsinate ($(CH_3)_2AsOONa$, NaCac - Carlo Erba, 96% purity) were prepared by dissolving weighed amounts of the solid in water and titrated with NaOH. To reliably reproduce the ionic strength near physiological conditions, the ionic strength (I) of the working solutions was kept constant at 0.1 M with sodium perchlorate (Merck), whereas the desired pH was attained by addition of small amounts of NaOH and $HClO_4$. $NaClO_4$ was chosen as the ionic buffer because perchlorate is an inert anion,[20] whereas other species such as chloride and phosphate can form complexes with Al(III).[21] All of the reactants were analytical grade and were used without further purification. Ultra-pure water from a Millipore MILLI-Q water purification system was used to prepare the solutions and as a reaction medium.

2.2. Methods

pH measurements were performed with a Metrohm 713 (Herisau, Switzerland) pH-meter equipped with a combined glass electrode. Aluminium samples were not so stable as those with only the buffer and based on several repeated measurements, we have stated the pH uncertainty to 0.05. The pH values measured in D_2O were not corrected for isotope effect as long as data on D_2O at high acidity levels is lacking. Spectrophotometric titrations were carried out with a Shimadzu 2450-Spectrophotometer, equipped with jacketed cell holders (thermostat precision 0.1 °C). All experiments were conducted at 25 °C. Titrations of Al(III)/Cac system were performed in the batch-wise mode at the desired pH values and ionic strength 0.1 M ($NaClO_4$). Different samples were

prepared for different metal-to-ligand ratios and left for 24 h to achieve equilibration. The absorbance spectrum for each sample was recorded in the 190-300 nm range (1 cm path-length cells) and the binding parameters were evaluated averaging out the results obtained at different selected wavelengths in the 205-193 nm range. Mass spectra were recorded by means of a TOF Mass Spectrometer Bruker Maxis Impact with electrospray ionization (ESI) for C_L/C_M = 1 (C_M = 0.2 mM) samples in double distilled water, C_L and C_M being the cacodylate and aluminium ion concentrations, respectively. NMR samples were prepared by dissolving the proper amount of Al^{3+} in 0.5 mL of the respective oxygen-free deuterated solvent to 5 mM working solutions with the corresponding amount of Sodium Cacodylate for each C_L/C_M ratio studied. Unless otherwise stated, the spectra were recorded at 298 K on a Varian Unity Inova-400 (399.94 MHz for ^{1}H; 104.21 MHz for ^{27}Al). Typically, 1D ^{1}H NMR spectra were acquired with 32 scans into 32 k data points over 16 ppm spectral width; the spectra of ^{27}Al NMR were acquired with 16 scans. ^{1}H chemical shifts were referenced internally to TMS via 1,4-dioxane in D_2O (δ = 3.75 ppm). Chemical shift values are reported in ppm. The NMR data processing was carried out using MestReNova version 6.1.1.

DFT calculations were carried out using B3LYP functional to optimize some proposed structures for the aluminium-sodium cacodylate complex; this procedure was used satisfactorily for DFT calculations of metals,[22] and specifically for aluminium,[23-25] applying 6-31G(d) basis set to C, H and O atoms. A double zeta function (LANL2DZ) was used for Al and As, including effective core potential calculation (ECP) for core electrons, diminishing the computational calculation costs. Water was used as solvent. All calculations and data analyses were performed with Gaussian 09.[26]

3. Results and Discussion

3.1. Evaluation of the $pK_{A,1}$ and $pK_{A,2}$ acidity constants of cacodylic acid

Cacodylic acid is a diprotic acid; its diprotonated form is denoted here as H_2Cac^+. This species undergoes acid dissociation according to eqns (1) and (2), which characterize the acid dissociation constants $K_{A,1}$ and $K_{A,2}$, respectively.

$$H_2Cac^+ + H_2O \rightleftarrows HCac + H_3O^+ \quad (1)$$

$$HCac + H_2O \rightleftarrows Cac^- + H_3O^+ \quad (2)$$

The ^{1}H-NMR spectrum of cacodylate shows a singlet signal ascribable to the methyl groups of NaCac. The location of these peaks very much depends on the medium acidity, for the higher the acidity level the larger the chemical shift of the peaks (Fig. 1A).

The $pK_{A,1}$ and $pK_{A,2}$ values have been determined by analyses of the chemical shift of the ^{1}H-NMR singlets of sodium cacodylate at different values of pH and acidity function H_0 (Fig. 1B); the latter function was employed at the highest acidity levels used, outside the boundary of the pH scale.[27] The two dissociation constants of cacodylic acid were evaluated according to eqn (3):

$$\delta = \frac{\delta_B - \delta_{BH^+}}{1+10^{-pH+pK_{A,i}}} + \delta_{BH^+} \quad (3)$$

where δ_B and δ_{BH+} represent the chemical shift of the basic and acidic forms, respectively, and δ that at an intermediate acid concentration, according to species shown in eqns (1) and (2). To determine $pK_{A,1}$, eqn (3) was applied directly adopting for δ_B the chemical shift at pH = 4, whereas that for δ_{BH+} was taken as the highest value in Fig. 1B. The continuous line denotes the outcome of the two fittings. The $pK_{A,1}$ and $pK_{A,2}$ values obtained, 1.3 ± 0.2 and 6.2 ± 0.1 respectively, were in reasonable good agreement with literature values, $pK_{A,1}$ = 1.1[10, 28] and 2.6[28], and $pK_{A,2}$ = 6.2.[10-13] Fig. 1C shows the speciation curves of cacodylic acid.

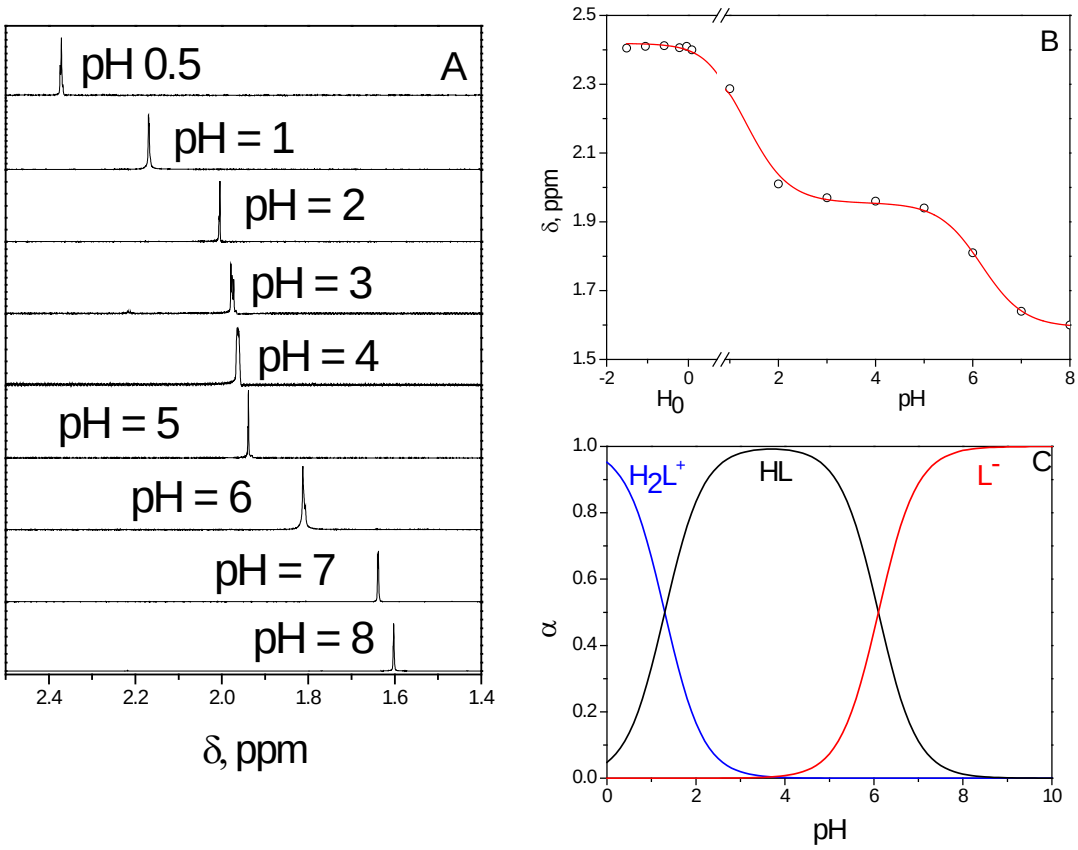

Fig. 1 (A) ^{1}H-NMR spectra at pH= 0.5, 1, 2, 3, 4, 5, 6, 7 and 8. (B) δ versus pH (or H_0) plot corresponding to $pK_{A,1}$ and $pK_{A,2}$. $C_L = 5.00 \times 10^{-3}$ M. (C) Speciation of cacodylic acid ($pK_{A,1} = 1.3$, $pK_{A,2} = 6.1$). I = 0.1 M ($NaClO_4$), T = 25.0 °C.

As for the absorbance measurements, Fig. S1 (ESI) shows the spectra of cacodylic acid at different pH values (I = 0.1 M, $NaClO_4$). The change in absorbance upon titration within the 2-10 pH range (Fig. S1, inset) has enabled us to evaluate the second acid dissociation constant of cacodylic acid, $pK_{A,2} = 6.0 \pm 0.2$. A point worthy of mention is that the absorption spectra of cacodylate lie in the limit of the instrumental range, and the measure suffers low signal-to-noise ratio. Therefore, to ensure reliable results, $K_{A,2}$ was calculated at every wavelength in the 195-205 range. The mean values obtained in this range were within the experimental error. Below pH 3, the observed shift to lower wavelengths of the 193 nm band can be ascribed to formation of the H_2Cac^+ species.

3.2 Speciation of aluminium forms

Fig. 2 shows the ^{27}Al-NMR spectra in the 1–6 pH range (above pH 6, measurements could not be performed because aluminium precipitates). NMR measurements show that the hexaaquoaluminium (III) ion, $Al(OH)_6^{3+}$, prevails between pH 1 and 4. The wide band in ^{27}Al-NMR spectra observed between pH 5 and 6 can be ascribed to the polycation species $Al_{13}O_4(OH)_{24}^{7+}$ (also denoted as Al_{13}-mer).[29] Between pH 6 and 7, partial or full neutralization of the polymer charge promotes aggregation of Al_{13}-mer, which tends to precipitate, and formation of more complex polymeric forms, such as $Al_2O_8Al_{28}(OH)_{56}(H_2O)_{26}^{18+}$ (also known as Al_{30}-mers) is likely to occur.[30, 31]

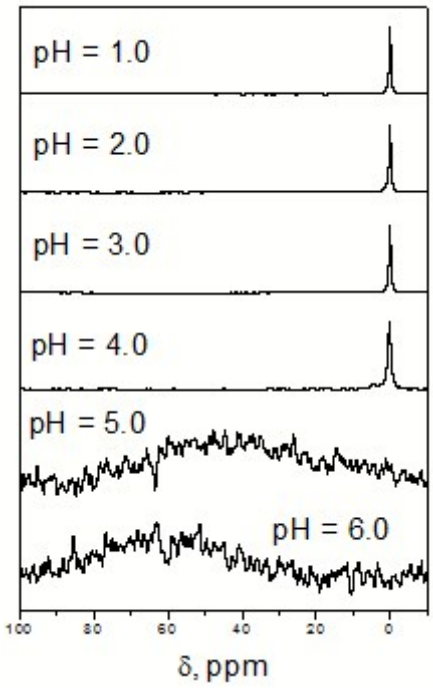

Fig. 2 ^{27}Al-NMR spectra of Al(III) at different pH values. C_M = 5.00 × 10^{-3} M, I = 0.1 M ($NaClO_4$) and T = 25.0 °C. The pH-independent narrow peak at (roughly) δ 0 ppm, is ascribed to the monomeric species Al^{3+}, whereas the broad band observed at pH 5 and 6 corresponds to the $Al_{13}O_4(OH)_{24}^{7+}$ polymer.

The NMR findings are corroborated by literature data. The molar fraction (β) of the Al^{3+} hexahydrate ion and its hydrolytic forms can be calculated according to eqn (4):[1]

$$\mathrm{LogQ_{xy}} = \mathrm{LogK_{xy}} + \mathbf{a}\frac{\sqrt{\mathrm{I}}}{1+\sqrt{\mathrm{I}}} + \mathbf{b}\mathrm{m_x} \qquad (4)$$

where I is the ionic strength of the medium, Q_{xy} is the equilibrium ratio related to formation of the hydrolyzed $Al_x(OH)_y^{(3x-y)+}$ species ($xAl + yH_2O \leftrightarrows Al_x(OH)_y^{(3x-y)+} + yH^+$), K_{xy} is the relevant thermodynamic equilibrium constant, and m_x is the overall aluminium molality, ***a*** and ***b*** being fitting parameters.[1] This calculation was performed at different pH values and metal concentrations using the Octave program,[32] yielding the distribution plots shown in Fig. 3. This figure shows that the amount of dimer and trimer species is negligible and that the predominant species in the 4.5 to 8.0 pH range is $Al_{13}O_4(OH)_{24}^{7+}$, whereas $Al(OH)_4^-$ is the prevailing species above pH 8.0.

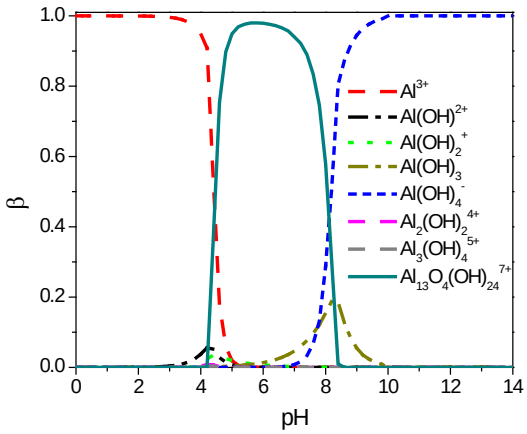

Fig. 3 Speciation of Al(III). $C_M = 1.00 \times 10^{-3}$ M, I = 0.1 M and T = 25.0 °C.

The results from Fig. 3 are compared in Fig. S2 (A and B, ESI) with other results obtained for Al^{3+} concentrations of 1.0×10^{-4} and 1.0×10^{-5} M, showing that in dilute solutions polymeric species are absent. Additionally, an increase in the aluminium concentration (C_M) causes a modest diminution of β_{Al}^{3+} and a sharp increase in the polymeric form $Al_{13}O_4(OH)_{24}^{7+}$.

3.3. The aluminium/cacodylate system

Mass spectrometry. The different number of peaks recorded at different pH values reveals the complexity of the distribution of the aluminium species (Fig. S3, ESI). We focused the attention on the most representative peaks in the spectrum and determined four types of species: **(1)** free

cacodylate, which is predominant and, in particular, the $[HCac + H]^+$ (m/z = 139) and $[NaCac + H]^+$ (m/z = 161) adducts and other peaks reported in literature,[33,34] such as m/z = 277, 259, 299, 281, 437 and 419 (corresponding to $[H_2Cac_2+H]^+$, $[H_2Cac_2+H-H_2O]^+$, $[H_2Cac_2+Na]^+$, $[H_2Cac_2+Na-H_2O]^+$, $[H_3Cac_3+Na]^+$, $[H_3Cac_3+Na-H_2O]^+$), respectively; **(2)** perchlorate and cacodylate salt clusters: $[Na(NaClO_4)_x]^+$ (m/z = 145, 267, 389) and $[Na(NaCac)_x]$ (m/z = 183, 343, 503, 663); **(3)** Al non-complexed forms: $Al(OH)_2(H_2O)_v^+$ (m/z = 79, 115, 133); $Al_2O(OH_2)_3^+$ (m/z = 121) and **(4)** Al/Cac complexes. By analogy with the formulation of aluminium(III) of aquo-chloro-complexes, we adopt the general formula $Al_xO_y(OH)_zCac_u(H_2O)_v^{n+}$ for the aluminium/cacodylate complexes.[35] The distribution of the different forms is shown in Fig. 4, whereas the respective formulas are summarized in the Electronic Supporting Information (Table 1 ESI).

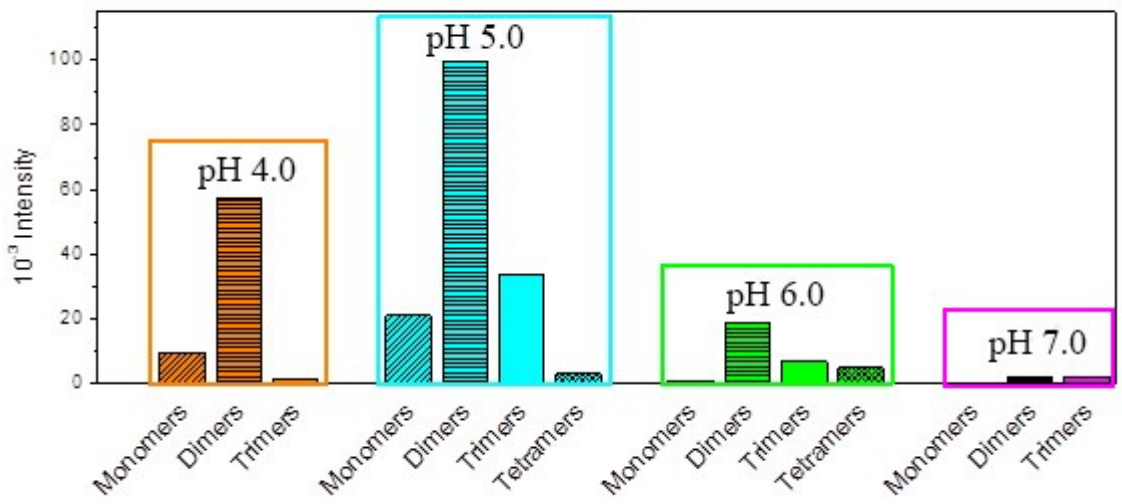

Fig. 4 Distribution of the different Al/Cac complex forms at different pH. $C_L = C_M = 2.00 \times 10^{-4}$ M and T = 25.0 °C.

It should be pointed out here that assignment of the proper formula is prone to certain degree of ambiguity.[36] To a first place, the $(OH)_2^{2-}$ and $O(OH_2)^{2-}$ patterns, having the same value of the m/z ratio, cannot be differentiated. Therefore, $Al_2O(OH)Cac_2(H_2O)^+$ could be replaced by $Al_2(OH)_3Cac_2^+$. Moreover, some peaks can be assigned to either a free or a bound aluminium

species. For instance, the peak at m/z = 121 can be ascribed to the free species $Al_2O(OH)_3^+$ and to the $Al_2O(OH)Cac(H_2O)_v^{2+}$ complex, and the peaks at 301 and 319 to the 1:2 complex $AlCac_2(H_2O)_v^+$ or to the 3:1 complex, $Al_3O(OH)Cac(H_2O)_v^+$. The theoretical and literature data (see below) will allow us put forward the most stable form.[35-39]

At pH 4.0, 5.0 and 6.0 the most intense peaks are those associable to the dimeric forms. On the other hand, monomeric species are mainly present not only at pH 5, but also at pH 4. Trimeric forms display lower intensity signals and are detected at pH 5.0, 6.0 and 7.0. In particular, the signal at pH 7.0 is lower than those detected at pH 5.0 and 6.0, concurrent with the weakening of the interaction of cacodylate at neutral pH, observed in the NMR experiments, as described below.

The high abundance of dimeric complexes contrasts with the β values, indicating rather modest presence of dimers when cacodylate is absent (Fig. 3). To support this view, previous studies[35-39] on aluminium complexes with organic ligands have shown that $Al_2O(OH)_3^+$ yields a small peak, suggesting that the dimeric aluminium free species are only poorly present in solution. Hence, it can be surmised that, in addition to the 1:1 complex, the presence of cacodylate induces formation of dimeric and (to a lesser extent) also trimeric and tetrameric species. Furthermore, the observation that the peaks of these species are present also at pH 5.0 and 6.0 (where in the absence of ligand the polymeric Al_{13}-mer form prevails by far), suggests that the ligand induces splitting of Al_{13}-mer to give smaller entities.

^{27}Al-NMR and ^{1}H-NMR studies. Fig. 5A shows the ^{27}Al-NMR spectra for Al/Cac in the pH 1 – 7 range. Between pH 1.0 and 2.0, only the signal corresponding to free Al^{3+} was observed at 0 ppm. In addition to the signal at 0 ppm, at pH 3.0 and 4.0 two further signals were observed at 2 and 4 ppm, the former remaining very modest at the two pH values. The second displays a remarkable increase in intensity on going from pH 3.0 to pH 4.0. At pH 5.0 and 6.0, wide bands were observed at 8 and 12 ppm, respectively. At pH 7.0, the centre of the band is shifted to 60 ppm.

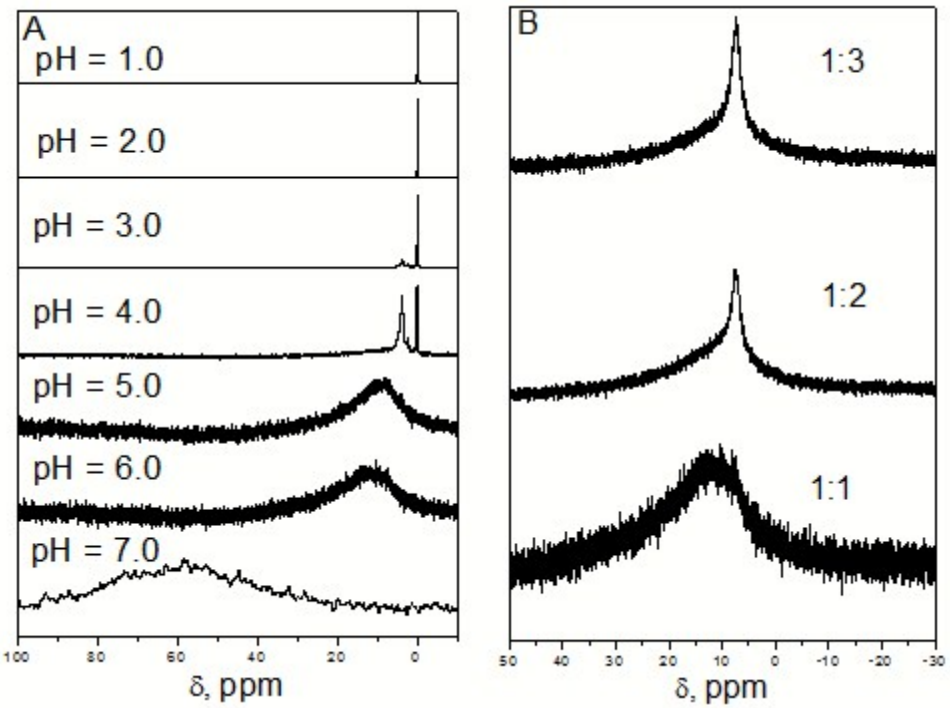

Fig. 5 ^{27}Al-NMR spectra for (A) Al/NaCac system at pH = 1.0, 2.0, 3.0, 4.0, 5.0, 6.0 and 7.0, C_M/C_L = 1:1 (B) Al/NaCac system at C_M/C_L = 1:1, 1:2 and 1:3, $C_M = 5.00 \times 10^{-3}$ M, pH = 6.0, I = 0.1 M ($NaClO_4$) and T = 25 ºC.

Fig. 6 shows the ^{1}H-NMR spectra of the Al/NaCac system recorded at different pH values and different times. The peak of the free ligand (circled δ), and other peaks are displayed in the 4 ≤ pH ≤ 7 range, which are associated to bound cacodylate. The whole of the ^{27}Al-NMR and ^{1}H-NMR experiments have contributed to interpret the behaviour of the aluminium/cacodylate system at different pH values. No Al/Cac complex is formed at pH 1.0 and 2.0. However, small amounts of complex are detected at pH 3.0 and the extent of binding becomes more and more important as the pH is raised, in agreement with the general behaviour displayed by complex formation reactions of metal ions with ligands protonated at the reaction site.

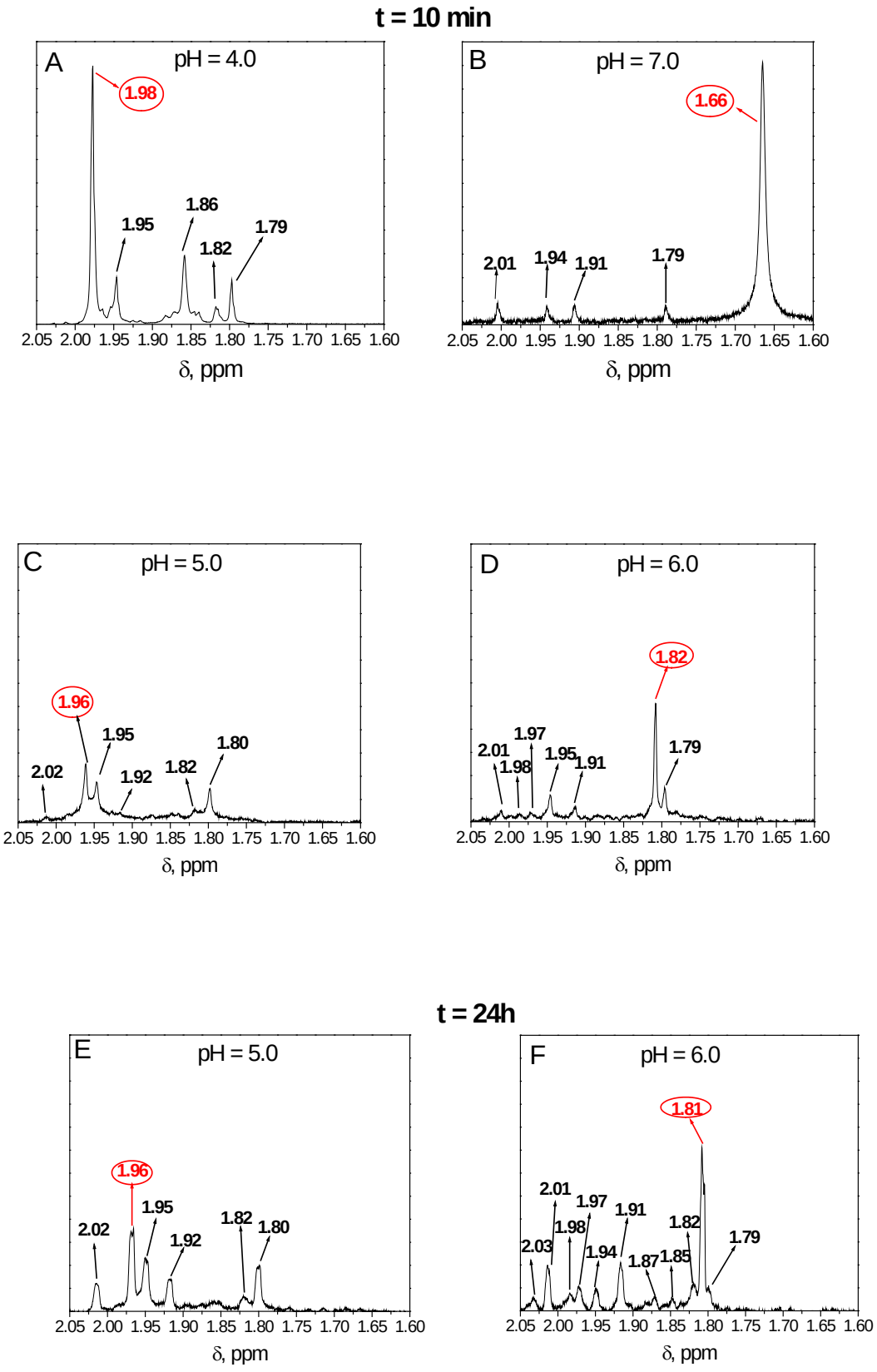

Fig. 6 ^{1}H-NMR kinetics of Al/NaCaC complex at t = 10 min (A, B, C and D) and t = 1 day (E and F). $C_M = C_L = 5.00 \times 10^{-3}$ M, I = 0.1 M ($NaClO_4$), pH = 4.0–7.0 and T = 25 °C. Circled chemical shift stands for free cacodylate at every pH.

Concerning the data at pH 4.0, comparison of the ^{27}Al-NMR spectra of free (Fig. 2) and bound (Fig. 5A) aluminium shows a remarkable increase of the peak at 4 ppm, which can be associated to the dimeric aluminium/cacodilate form.[40,41] In the ^{1}H-NMR spectrum (Fig. 6A), the singlet at 1.86 ppm could be related to the $AlCac^{2+}$ complex. Actually, the beta value of Al^{3+} at pH 4.0 is 0.9, and a singlet peak is in agreement with the Al^{3+} symmetrical form with the chelating ligand. In addition, it is supported by the fact that this peak is not seen at pH 5.0 (Fig. 6C), where β_{Al3+}=0.004. The two peaks at 1.95 and 1.79, having the same intensity, most likely correspond to a dimeric form, in which the two methyl groups have different environment. Also other small peaks are present, in particular in the 1.88-1.85 ppm range and at 1.82 ppm, which **could** be related to other monomeric species, such as $Al(OH)Cac^{+}$.

The broad peak observed at pH 5.0 and 6.0 in the ^{27}Al-NMR experiments (Fig. 5A) should be associated to the sum of dimeric, trimeric and other polymeric species arising from decomposition of the Al_{13} aggregate associated to the broad peak at 60 ppm (Fig. 2). In addition, ^{27}Al-NMR spectra recorded at pH 6.0 for C_L/C_M 1, 2 and 3 show constriction of the broad peak, with signal increase at 7.5 ppm (Fig. 5B). This behaviour agrees well with further splitting of the Al_{13}-mer in the presence of an excess of cacodylate. As stated above, the ^{1}H-NMR experiments show that the peak at 1.86 ppm, present at pH 4.0, disappears when the solution pH is raised (spectra at pH 5.0 and 6.0 in Figs. 6C and 6D), while the peaks at 1.95 and 1.80 ppm exhibit remarkable intensity. Moreover, a very slow kinetic process is observed, followed by the increase of two peaks at 2.01 and 1.92 ppm of same intensity (Figs. 6E and 6F). Therefore, we can surmise that the interaction between aluminium and cacodylate is the summation of two reactions. The first one is fast, possibly representing the ligand binding to monomeric or dimeric aluminium species, and the second represents the decomposition of the polymeric Al_{13}-mer induced by interaction of cacodylate to give simpler species, in agreement with the observed disaggregation of Al_{13}-mer induced by ligands with oxygen-containing groups, such as acetate, oxalate and lactate and, more

conceivably, by protons.[31, 42-44] In this case, disaggregation seems to be strongly dependent on the pH and less on the ligand nature.

Furrer et al.[42] state that disaggregation of Al_{13}-mer is driven by proton concentration. In other words, the only presence of cacodylate does not justify by itself disaggregation of the aluminium oligomers under the experimental conditions (C_L/C_M = 1). However, ^{1}H NMR spectra (Fig. S4, ESI) show that excess of ligand causes an increase in the peak intensity associated to complexed cacodylate. Thus, certain competition between the inner and outer coordination spheres can be envisaged in excess of ligand, where the former can evolve to simpler forms by disruption of the polymer. The results at pH 7.0 significantly differ from the trend observed at pH 5.0 and 6.0. A very broad, low intensity, peak centred at 60 ppm is obtained in ^{27}Al-NMR spectra (Fig. 5A), and the ^{1}H-NMR exhibits very small peaks of the complexed forms (Fig. 6B), even at same resonance of the peaks at pH 5.0 and 6.0. However, at pH 7.0 no precipitation was observed in Al/Cac solutions, whereas extended precipitation occurs for free aluminium. Therefore, we can assume occurrence of interaction, although of different nature compared to that at work at lower pH values.

Stumm[45] suggested that the interaction of an organic ligand with a solid interface can be differentiated between inner (strong bonding) and outer (weak bonding) coordination sphere. In a study of the acetate/aluminium system[46] it was proposed that the interaction of the acetate ion with Al_2O_3 in suspension involves mainly the outer coordination sphere. We suggest that at pH 7.0 cacodylate can interact with Al(III) aggregates in the same way as acetate reacts with aluminium oxide suspension. The resulting complex enables aluminium to remain in solution. This result is interesting because we verified that cacodylate renders aluminium soluble near physiological conditions systems (I = 0.1 M, pH = 7.0 and T = 25.0 ºC).

Determination of K_{app} of aluminium/cacodylate complexes. The apparent equilibrium constant, K_{app}, for formation of the aluminium/cacodylate (Al/Cac) complexes, was determined

from batch-wise spectrophotometric titrations performed for different pH values. The apparent reaction is,

$$M_f + L_f \leftrightarrows ML_T \quad (5)$$

where M_f and L_f are the non-complexed free metal and ligand forms, respectively, and ML_T is the total complex. Most of the experimental data-pairs were obtained with no excess of metal or ligand. The interaction between aluminium species and cacodylate causes a hypochromic effect (Fig. 7A). The data-pairs were analysed according to eqn. (6):

$$\frac{C_L C_M}{\Delta A} + \frac{\Delta A}{\Delta \epsilon} = \frac{C_L + C_M}{\Delta \epsilon} + \frac{1}{K_{app} \Delta \epsilon} \quad (6)$$

where C_L and C_M are the analytical ligand and metal concentration, respectively, $\Delta A = A - \varepsilon_L C_L$ and $\Delta\varepsilon = \varepsilon_{ML} - \varepsilon_L$, where ε_i is the absorptivity of the i^{th} species.

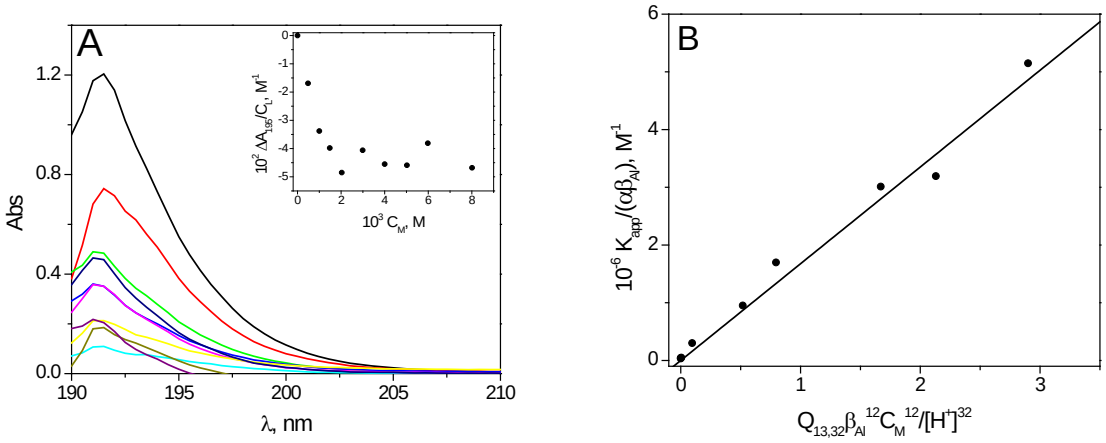

Fig. 7 (A) Example of spectrophotometric titration of the Al/Cac system. Inset: track at λ = 195 nm. $C_L = 1.0 \times 10^{-3}$ M, I = 0.1 M, pH = 4.8 and T = 25.0 °C. (B) Analysis according to eqn (8) of the 4.3 < pH < 5.0 data.

Different binding isotherms were obtained using absorbance values within 195-205 nm (Fig. 7A), a range where aluminium ion displays no absorption, whereas the different dimethylarsinic forms have different absorptivity, ε_i. As for the $pK_{A,2}$ constant of free cacodylate calculated by UV-Vis, use of different tracks reinforces the goodness of our results. The equilibrium constants

obtained (Table 1) are averaged values. At pH = 2, such evaluation was unfeasible because the change in absorbance was too modest owing to the repression of the binding reaction caused by protons, in agreement with the NMR results.

Table 1. Apparent equilibrium constant for binding of aluminium to cacodylate (K_{app}) at different pH. I = 0.1 M and T = 25 °C.

pH	K_{app} (M^{-1})
3.0	25±5
4.0	290±50
4.3	560±60
4.5	2200±300
4.7	3400±600
4.8	4600±900
4.9	5400±1000
5.0	6500±1000

The relationship between K_{app}, and $[H^+]$ is expressed by eqn (7) (see ESI) in the form:

$$\frac{K_{app}}{\alpha_L \beta_{Al}} = K^I + K^{II}\frac{Q_{1.1}}{[H^+]} + K^{III}\frac{Q_{1.2}}{[H^+]^2} + K^{IV}\frac{Q_{1.3}}{[H^+]^3} + K^{V}\frac{Q_{1.4}}{[H^+]^4} + \\ + K^{VI}\frac{Q_{2.2} C_M \beta_{Al}}{[H^+]^2} + K^{VII}\frac{Q_{3.4} C_M^2 \beta_{Al}^2}{[H^+]^4} + K^{VIII}\frac{Q_{13.32} C_M^{12} \beta_{Al}^{12}}{[H^+]^{32}} \quad (7)$$

where α_L is the mole fraction of the species Cac^-, β_{Al} is the mole fraction of the species Al^{3+}, K^I, K^{II}, K^{III}, K^{IV}, K^V, K^{VI}, K^{VII} and K^{VIII} are the true thermodynamic constants for binding of Cac to Al^{3+}, $Al(OH)^{2+}$, $Al(OH)_2^+$, $Al(OH)_3$, $Al(OH)_4^-$, $Al_2(OH)_2^{4+}$, $Al_3(OH)_4^{5+}$ and $Al_{13}O_4(OH)_{24}^{7+}$, respectively. On the other side, the β values (Fig. 3) support simplification of eqn (7) to eqn (8). Actually, except for Al^{3+} and Al_{13}-mer, all contributions are negligible under the experimental conditions employed, the mole fraction of the other species being low.

$$\frac{K_{app}}{\alpha_L \beta_{Al}} = K^I + K^{VIII}\frac{Q_{13.32} C_M^{12} \beta_{Al}^{12}}{[H^+]^{32}} \quad (8)$$

Moreover, since formation of the polymeric form is fully attained within a very narrow pH range, two well defined pH ranges can be distinguished. In the first range (3.0 < pH < 4.3), the

monomers Al^{3+} and $AlOH^{2+}$ are active, while in the second ($4.7 < pH < 5.0$) the Al_{13}-mer is active. For $pH > 4.5$, the contribution of K^I to eqn (8) is negligible (Fig. 7B). In this pH range, $\log[K_{app}/(\alpha_L\beta_{Al}{}^{13})]$ *versus* pH plots for different C_M values (Fig. S5 A, ESI), and $\log[K_{app}[H^+]^{32}/(\alpha_L\beta_{Al}{}^{13})]$ *versus* C_M plot (Fig. S5 B, ESI) yielded straight lines with slope equal to 32 and 12, respectively, reinforcing the presence of $Al_{13}O_4(OH)_{24}{}^{7+}$ as the reactive species. Analysis according to eqn (8) of K_{app} *versus* pH plots yielded $K^{VIII} = (1.6 \pm 0.4) \times 10^6\ M^{-12}$ (Fig. 7B). This data can be used in the $3.0 < pH < 4.3$ region to evaluate the true thermodynamic constant $K^I = (4 \pm 2) \times 10^4\ M^{-1}$.

Likewise, from the NMR data obtained we evaluated the apparent equilibrium constant for $C_L = C_M$ and different pH values (see ESI). The K_{app} values obtained at pH 4 and 5 (Table 1 ESI) concur well with the spectrophotometric values (Table 1). However, the values obtained at pH 6 and 7 are smaller than expected, thus disagreeing with the model proposed by UV measurements (Fig. 6 ESI) due to the observed aggregation trend of the Al_{13} units. The ^{27}Al-NMR results show that the interaction between metal and ligand yields the AlCac complex and not AlHCac or AlH_2Cac, however no indication was inferred as to forming AlCac from reactions (9) or (10):

$$Al^{3+} + Cac^- \leftrightarrows AlCac^{2+} \qquad (9)$$

Reaction (9) cannot be distinguished from the equivalent reaction (10), neither by thermodynamic experiments (since the dependence of the conditional equilibrium constant on $[H^+]$ would be the same) nor kinetically (since the formula of the activated complex would be the same):

$$AlOH^{2+} + HCac \leftrightarrows AlCac^{2+} \qquad (10)$$

Careful consideration of the kinetic behaviour of Al(III) species have allow us establish the most probable pathway: being $AlOH^{2+}$ about 10^4-fold more reactive than Al^{3+} aquo ion (as it follows from comparison of the respective rates of water exchange[47]) the first step of the Al(III) binding to a chelating ligand should be about 10^3-fold faster in the case of $AlOH^{2+}$.[48] Hence, for pH

> 2 the formation of $AlCac^{2+}$ will proceed mainly through reaction (10). The equilibrium constant of reaction (10), denoted as $K^{I'}$, is related to K^{I} by the relationship $K^{I'} = K^{I}K_{A2}/Q_{11}$. Its value is $K^{I'} = (8 \pm 4) \times 10^{3}$ M^{-1}. Only for pH > 5 the contribution of the deprotonated Cac^{-} ion to the binding reaction becomes important. This interpretation differs from that advanced in a previous study,[19] were the formation of the 1:1 complex was rationalized assuming that the main process is the reaction of the Al^{3+} ion with the deprotonated form of the ligand, Cac^{-}.

DFT calculations: hypothesis of Al/Cac structures. By means of mass spectrometry and NMR data, we have hypothesized possible Al/Cac structures. It can reasonably be assumed that the ligand chelates the metal, as demonstrated for other oxygenated ligands with aluminium.[31, 46, 49]

The suggested structure of the monomer species is shown in Fig. 8A (note that water molecules can be replaced by hydroxo groups, and more than one ligand could be present). For the dimer species, the mass spectrometry and NMR data gathered do not clarify the exact structure, so different geometries can be considered. Based on earlier studies on different Al(III) complexes,[36, 46] we propose the following structures: two aluminium atoms linked by two oxygen groups (Fig. 8B); the interaction of the aluminium complexes is obtained via hydroxo groups (Fig. 8C), only one oxygen binds the aluminium complexes, like in the third structure (Fig. 8D). Interestingly, a different M_2L structure is proposed for the aluminium/acetate complex.[46] Since cacodylate has similar structure as acetate, we propose similar geometry associated to the most intense signal in the mass spectrometry (m/z = 121) and NMR (δ = 1.95 and 1.80 ppm) spectra (Fig. 8E). As a matter of fact, a *syn-syn* bridging geometry is considered by the experimental results, where the two oxygens bind to both aluminium atoms of the dimeric form. Hence, a double hydroxo- or oxo- bridged geometry is present. For the trimeric and tetrameric species, other more complex structures can be hypothesized with the same bridging geometry.

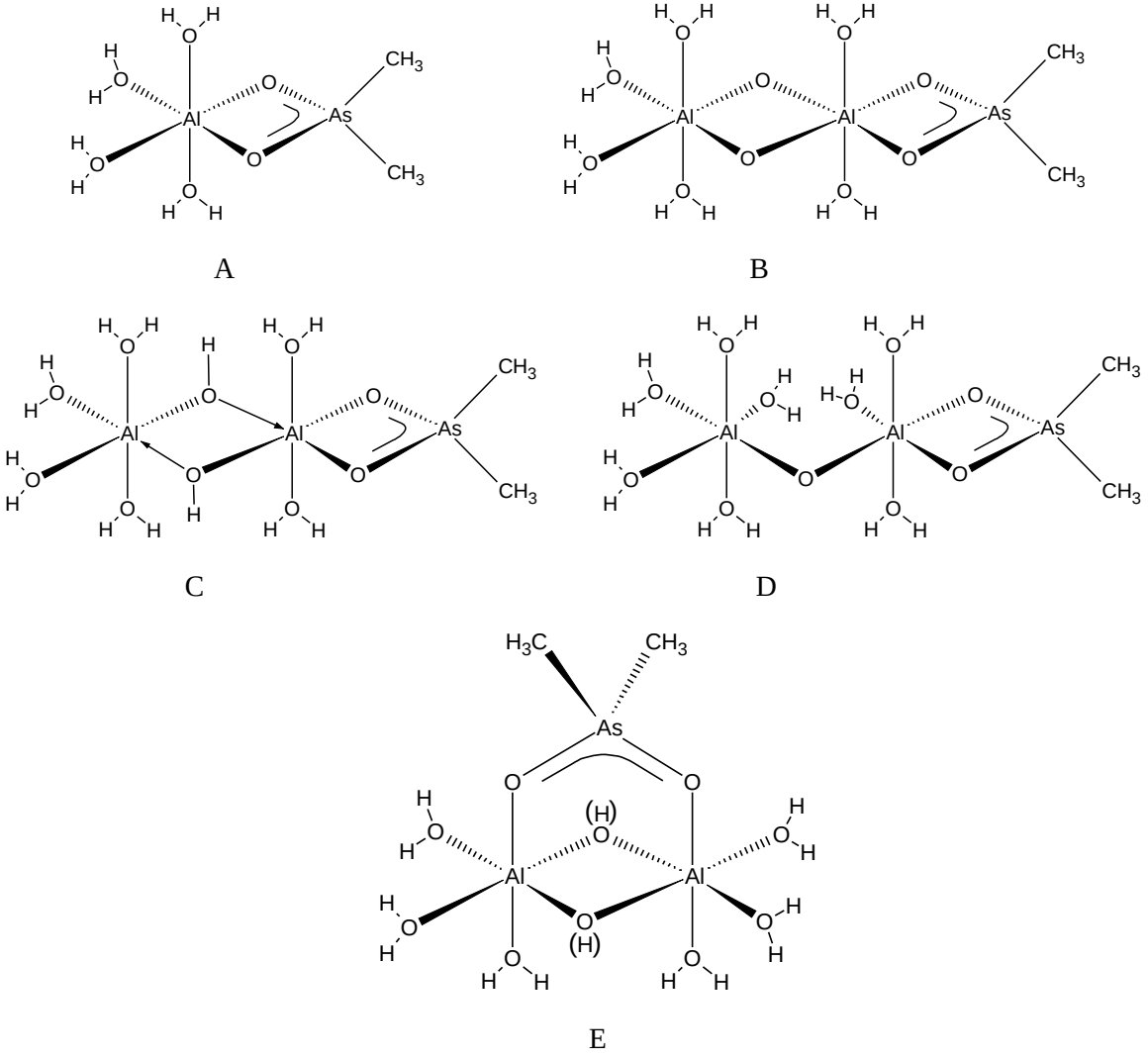

Fig. 8 (A) 1:1 structure. (B) First 2:1 structure. (C) Second 2:1 structure, (D) Third 2:1 structure (E) Fourth 2:1 structure: *syn-syn* bridging geometry.

To convincingly justify the hypotheses drawn on the dimeric complexes, we undertook theoretical energy calculations of these complexes. For the M_2L dimeric system, four different structures were calculated (B,C and two more E structures, with and without bridging oxygens, which will be denoted as E(OH) and E(O), respectively. The two E structures consist of a 2:1 complex, where Cacodylate is bound to only one Al atom via a double O-bridge. B and C structures resemble the E(O) and E(OH) structures, respectively, but with OH bridging ligands between Al atoms, instead of O-bridge, and two more hydroxo ligands.

The stability has been studied in terms of the overall energy (products energy). The DFT optimization of these structures results in the following stability sequence, from most to least stable (Hartree units): (B) (-849.660435) > (C) (-849.651503)> (E(O)) (-849.590124) > (E(OH)) (-849.558751). Thus, the most stable structure involves OH-bridging ligands between Al atoms with cacodylate bound to both metal centres. The optimized structure of (E(OH) is plotted in Fig. 9A.

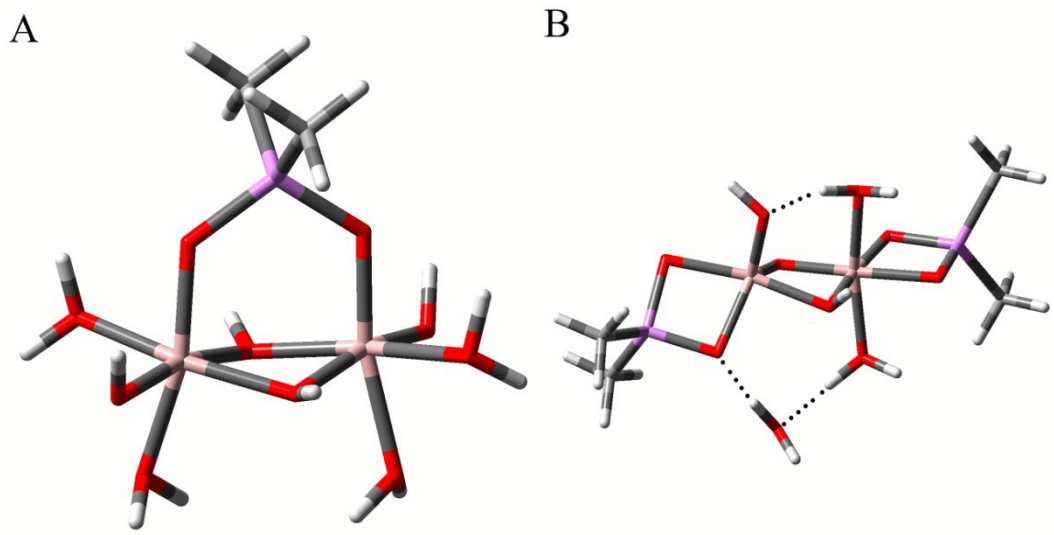

Fig. 9 (A) DFT optimization of E(OH) structure in water, using B3LYP functional with 6-31G(d) basis set for C (grey), H (white) and O (red) atoms, and LANL2DZ for Al (pink) and As (purple) atoms. (B) DFT optimization of 2:2 linear complex in water, using B3LYP functional with 6-31G(d) basis set for C(grey), H(white) and O(red) atoms, and LANL2DZ for Al (pink), As (purple) atoms and H-bonding interactions (dashed lines).

A non-symmetrical conformation has been obtained (C1 symmetry group) with OH groups in the Al-Al plane pointing to cacodylate group. Surprisingly, methyl groups bound to As adopted eclipsed conformation. Full NBO (Natural Bond Orbital) analysis has revealed, as expected, that the Al and As sites are primarily positively charged. Oxygen atoms in the Al-O-As bonds are significantly more negative than the others due to the metals charge donating nature. Thus, the Oxygen site in the OH-bridges between Al atoms are, indeed, more negative than those on the water molecules. The characterization parameters (bond distance and angle) of the “core” of the molecule (every atom surrounding Al and As atoms) are compiled in Table S2, ESI. The two atom distances

and angles containing Al are similar, showing that the core lies in a symmetric environment and the abovementioned asymmetry is due to the slightly asymmetric conformation of the H_2O, OH and CH_3 groups.

In addition, DFT optimization and geometry analysis of two 2:2 complex structures (Fig. S7, ESI), has been carried out, whose presence was confirmed by mass spectrometry (m/z = 361). Since the calculations of a double *syn-syn* bridging geometry complex (Fig. S7 A, ESI) proved to be unstable in water, complex linear geometry (Fig. S7 B, ESI) has been DFT optimized to a minimum energy state (E= -933.31Hartrees). In the final conformation, one hydrogen atom from a water molecule is lost, and transferred to one of the O-bridging ligand between Al atoms. Moreover, a full water molecule is lost, remaining nearby the 2:2 complex via H-bonding interaction (Fig. 9B). These rearrangements, result in a surprisingly different conformation for Al atoms, from the initial Al(octhedral)-Al(octahedral) to Al(pyramidal)-Al(octahedral).

The stabilization of the pyramidal configuration can be explained by the H-bonding induced by the above mentioned water molecule that falls off the molecule (Table S3, ESI), showing that expected symmetry of the optimized structure is totally lost. The distance and angle values of the Al-O bonds considerably differ from their theoretical mirror image bonds. The dihedral angles show different orientation of the As-O-Al(pyramidal)-O and As-O-Al(octahedral) rings compared to the plane containing Al(1), O(2) and Al(3); the Al(pyramidal) ring is primarily orientated to the yz plane, whereas the Al(octahedral) containing ring, lies in the xz plane. As described for the 2:1 complex, the NBO analysis displays electron donation from metals to oxygen, an effect more intense for the O-bridging ligands between Al atoms.

DFT calculations suggest that the 2:2 complex hypothesized by MS data is an asymmetric system, in which the four methyl groups are surrounded by different chemical environment; then, it follows that they have different chemical shift. The ^{1}H-NMR spectra at pH = 6.0 (Fig. 6D) of the Al/Cac system show a number of peaks that, even if they cannot be specifically associated to the

corresponding methyl group, they could agree with a Al_2Cac_2 asymmetric system. At pH = 5.0 these peaks are only little visible, even if the MS spectra denote that Al_2Cac_2 is a relevant product. Regarding ^{27}Al-NMR, the broad peak observed does not allow obtaining information on the presence of this specific complex. However, other studies suggest the presence of penta-coordinated aluminium for oxygenated ligand and mono- and dimeric aluminium.[50, 51]

4. Conclusions

Thermodynamic experiments of the interaction between Al(III) and dimethylarsinic acid suggest that the apparent binding affinity has a maximum in the pH 5-6 region, whereas at pH 4.0 and pH 7.0 the binding strength is low. Comparison of the MS and NMR data suggests that the main species formed is a 2:1 complex. Thus, the most probable effect is that the 1:1 complex, which forms first, has a high affinity for a second aluminium ion. In particular, the most plausible structure is the dimeric *syn-syn* bridging geometry structure of cacodylate, interacting with the two aluminium centres (Fig. 8E). On the other hand, the different behaviour observed at pH 7.0 relative to that at pH 4-6 is explained assuming formation at neutral pH of an outer sphere coordination of the ligand to the Al_{13} aggregates, thus avoiding precipitation. On the other hand, at lower pH the polymeric form splits into smaller units, an effect promoted mainly by the proton and, to a less extent, by the ligand. Elucidation of the Al/Cac complex, which prevents aluminium from precipitation, in particular under near physiological conditions (I = 0.1 M, pH = 7.0 and 25.0ºC), can be very useful to obtain a system useful to study the biological processes and molecular mechanisms that underlie pathological effects induced by aluminium ions.

Acknowledgements

This work was supported by Obra Social “la Caixa” (OSLC-2012- 007), and MINECO, CTQ2014-58812-C2-2-R projects, Spain

Electronic Supplementary Information (ESI) available: Figs S1 to S7, Tables S1 to S3 and derivation of eqn 8. See DOI:

Notes and References

1. C. F. Baes and R. E. Mesmer, in *Hydrolysis of Cations*, John Wiley & Sons, New York1976, ch. 6, pp. 112-123.
2. M. Lamberti, I. D'Auria, M. Mazzeo, S. Milione, V. Bertolasi and D. Pappalardo, *Organometallics*, 2012, **31**, 5551-5560.
3. J. I. Mujika, J. M. Ugalde and X. Lopez, *Phys. Chem. Chem. Phys.*, 2012, **14**, 12465-12475.
4. S. Bhattacharjee, Y. Zhao, J. M. Hill, F. Culicchia, T. P. A. Kruck, M. E. Percy, A. I. Pogue, J. R. Walton and W. J. Lukiw, *J. Inorg. Biochem.*, 2013, **126**, 35-37.
5. T. Kiss, *J. Inorg. Biochem.*, 2013, **128**, 156-163.
6. A. Strunecka, R. L. Blaylock and J. Patocka, *Curr. Inorg. Chem.*, 2012, **2**, 8-18.
7. C. Exley and J. D. Birchall, *J. Theor. Biol.*, 1992, **159**, 83-98.
8. E. H. Jeffery, K. Abreo, E. Burgess, J. Cannata and J. L. Greger, *J. Toxicol. Env. Health*, 1996, **48**, 649-665.
9. S. A. Latt and H. A. Sober, *Biochemistry*, 1967, **6**, 3307-3314.
10. B. Holmberg., *Z. Phys. Chem.*, 1910, **70**, 153-158.
11. J. Juillard and N. Simonet, *Bull. Soc. Chim. Fr.*, 1968, 1883-1894.
12. K. B. Jacobson, B. D. Sarma and J. B. Murphy, *FEBS Lett.*, 1972, **22**, 80-82.
13. T. W. Shin, K. Kim and I. J. Lee, *J. Solution Chem.*, 1997, **26**, 379-390.
14. H. Diebler, F. Secco and M. Venturini, *Biophys. Chem.*, 1987, **26**, 193-205.
15. P. V. Ioannou, *Monatsh. Chem.*, 2012, **143**, 1349-1356.
16. P. V. Ioannou, *Z. Anorg. Allg. Chem.*, 2010, **636**, 1347-1353.
17. C. F. Whittemore and C. James, *J. Am. Chem. Soc.*, 1913, **35**, 127-132.
18. R. Pietsch, *Microchim. Acta*, 1958, 220-224.
19. P. V. Ioannou, *Monatsh. Chem.*, 2013, **144**, 793-802.
20. W. C. Wolsey, *J. Chem. Educ.*, 1973, **50**, A335-A337.
21. P. A. W. van Hees and U. S. Lundstrom, *Geoderma*, 2000, **94**, 201-221.
22. M. Lashkari and M. R. Arshadi, *Chem. Phys.*, 2004, **299**, 131-137.
23. H. Kawamura, V. Kumar, Q. Sun and Y. Kawazoe, *Mater. Trans.*, 2001, **42**, 2175-2179.
24. Z. J. Wu and X. F. Ma, *Chem. Phys. Lett.*, 2003, **371**, 35-39.
25. X. Jin, W. Yang, Z. Qian, Y. Wanga and S. Bi, *Dalt. Trans.*, 2011, **40**, 5052-5058.
26. M. J. Frisch, G. W. Trucks, H. B. Schlegel, G. E. Scuseria, M. A. Robb, J. R. Cheeseman, G. Scalmani, V. Barone, B. Mennucci, G. A. Petersson, H. Nakatsuji, M. Caricato, X. Li, H. P. Hratchian, A. F. Izmaylov, J. Bloino, G. Zheng, J. L. Sonnenberg, M. Hada, M. Ehara, K. Toyota, R. Fukuda, J. Hasegawa, M. Ishida, T. Nakajima, Y. Honda, O. Kitao, H. Nakai, T. Vreven, J. A. Montgomery, J. E. Peralta, F. Ogliaro, M. Bearpark, J. J. Heyd, E. Brothers, K. N. Kudin, V. N. Staroverov, R. Kobayashi, J. Normand, K. Raghavachari, A. Rendell, J. C. Burant, S. S. Iyengar, J. Tomasi, M. Cossi, N. Rega, J. M. Millam, M. Klene, J. E. Knox, J. B. Cross, V. Bakken, C. Adamo, J. Jaramillo, R. Gomperts, R. E. Stratmann, O. Yazyev, A. J. Austin, R. Cammi, C. Pomelli, J. W. Ochterski, R. L. Martin, K. Morokuma, V. G. Zakrzewski, G. A. Voth, P. Salvador, J. J. Dannenberg, S. Dapprich, A. D. Daniels, Farkas, J. B. Foresman, J. V. Ortiz, J. Cioslowski and D. J. Fox, Gaussian, Inc., Revision C.01 edn., 2010.
27. B. Garcia, S. Ibeas, F.J. Hoyuelos, J. M. Leal, F. Secco, M. Venturini, *J. Org. Chem.* 2001, **66**, 7986-7993.
28. M. L. Kilpatrick, *J. Am. Chem. Soc.*, 1949, **71**, 2607-2610.
29. G. Furrer, C. Ludwig and P. W. Schindler, *J. Colloid Interf. Sci.*, 1992, **149**, 56-67.

30. C. Ye, Z. Bi and D. Wang, *Colloid Surface A*, 2013, **436**, 782-786.
31. W. H. Casey, *Chem. Rev.*, 2006, **106**, 1-16.
32. J. W. Eaton, D. Bateman and S. Hauberg, in *A High-Level Interactive Language for Numerical Computations*, Create Space Independent Publishing Platform, 3.0.1 edn., 2009.
33. M. H. Florencio, M. F. Duarte, A. M. M. deBettencourt, M. L. Gomes and L. F. V. Boas, *Rapid Commun. Mass Sp.*, 1997, **11**, 469-473.
34. H. R. Hansen, A. Raab and J. Feldmann, *J. Anal. Atom. Spectrom.*, 2003, **18**, 474-479.
35. T. Urabe, M. Tanaka, S. Kumakura and T. Tsugoshi, *J. Mass Spectrom.*, 2007, **42**, 591-597.
36. A. Sarpola, V. Hietapelto, J. Jalonen, J. Jokela, R. S. Laitinen and J. Ramo, *J. Mass Spectrom.*, 2004, **39**, 1209-1218.
37. A. T. Sarpola, V. K. Hietapelto, J. E. Jalonen, J. Jokela and J. H. Ramo, *Int. J. Environ. An. Ch.*, 2006, **86**, 1007-1018.
38. A. Sarpola, V. Hietapelto, J. Jalonen, J. Jokela and R. S. Laitinen, *J. Mass Spectrom.*, 2004, **39**, 423-430.
39. T. Urabe, T. Tsugoshi and W. Tanakaa, *J. Mass Spectrom.*, 2009, **44**, 193-202.
40. J. W. Akitt and B. E. Mann, *J. Magn. Reson.*, 1981, **44**, 584-589.
41. J. J. Fitzgerald, L. E. Johnson and J. S. Frye, *J. Magn. Reson.*, 1989, **84**, 121-133.
42. G. Furrer, M. Gfeller and B. Wehrli, *Geochim. Cosmochim. Acta*, 1999, **63**, 3069-3076.
43. A. Masion, F. Thomas, D. Tchoubar, J. Y. Bottero and P. Tekely, *Langmuir*, 1994, **10**, 4353-4356.
44. A. Amirbahman, M. Gfeller and G. Furrer, *Geochim. Cosmochim. Acta*, 2000, **64**, 911-919.
45. W. Stumm, in *Chemistry of the solid-water interface: processes at the mineral-water and particle-water interface in natural systems*, John Wiley & Sons, New York1992, ch. 1, pp. 4-8.
46. P. Persson, M. Karlsson and L. O. Ohman, *Geochim. Cosmochim. Acta*, 1998, **62**, 3657-3668.
47. J. P. Nordin, D. J. Sullivan, B. L. Phillips and W. H. Casey, *Inorg. Chem.*, 1998, **37**, 4760-4763.
48. F. Secco and M. Venturini, *Inorg. Chem.*, 1975, **14**, 1978-1981.
49. R. B. Martin, *Clin. Chem.*, 1986, **32**, 1797-1806.
50. J. F. Stebbins, S. Kroeker, S. K. Lee and T. J. Kiczenski, *J. Non-Cryst. Solids*, 2000, **275**, 1-6.
51. C. H. Lin, B. T. Ko, F. C. Wang, C. C. Lin and C. Y. Kuo, *J. Organomet. Chem.*, 1999, **575**, 67-75.